

Abstract

late Eocene $p\text{CO}_2$ concentration is estimated based on the species of *Nageia maomingensis* Jin et Liu from the late Eocene of Maoming Basin, Guangdong Province. This is the first paleoatmospheric estimates for the late Eocene of South China using stomatal data. Studies of stomatal density (SD) and stomatal index (SI) with *N. motleyi* (Parl.) De Laub., the nearest living equivalent species of the fossil, indicate that the SD inversely responds to atmospheric CO_2 concentration, while SI has almost no relationships with atmospheric CO_2 concentration. Therefore, the $p\text{CO}_2$ concentration is reconstructed based on the SD of the fossil leaves in comparison with *N. motleyi*. Results suggest that the mean CO_2 concentration was 391.0 ± 41.1 ppmv or 386.5 ± 27.8 ppmv during the late Eocene, which is significantly higher than the CO_2 concentrations documented from 1968 to 1955 but similar to the values for current atmosphere indicating that the Carbon Dioxide levels during that the late Eocene at that time may have been similar to today.

1 Introduction

The Eocene (55.8–33.9 Ma) was characterized by much warmer temperatures than present-day, although temperatures also varied significantly across this time interval. Climate of the early Eocene to middle Eocene was extremely warm, particularly during the early Eocene Climatic Optimum (EECO; 52 to 50 Ma; Zachos et al., 2001), also known as the Paleocene–Eocene Thermal Maximum (PETM event; ~ 55.8 Ma; Wing et al., 2005; Kato et al., 2011). A series of sudden and extreme global warming events (hyperthermals; Deconto et al., 2012) have been described ~ 55.5 to 52 Ma; and a mid-Eocene warming has been recognized, the middle Eocene Climate Optimum (MECO; ~ 40 Ma; Bijl et al., 2010). However, the global climate occurred colder conditions during the early-middle (50 to 48 Ma) and the late Eocene (40 to 36 Ma; Zachos et al.,

CPD

11, 2615–2647, 2015

The $p\text{CO}_2$ estimates of the late Eocene in South China

X.-Y. Liu et al.

Title Page

Abstract

Introduction

Conclusions

References

Tables

Figures



Back

Close

Full Screen / Esc

Printer-friendly Version

Interactive Discussion



2001). The appearance of small-ephemeral ice-sheets during the latest Eocene suggests the coldest climate of the Eocene (Zachos et al., 2001).

Atmospheric CO₂ concentrations have been well correlated with global surface temperature change (Mann et al., 1998; Crowley, 2000; Barnett et al., 2001; Harries et al., 2001; Levitus et al., 2001; Mitchell et al., 2001). Most authors link the changes in temperature to atmospheric CO₂ concentration during the entire Phanerozoic (*p*CO₂) (Petit et al., 1999; Retallack, 2001; Royer, 2006). However, the Eocene *p*CO₂ record remains incomplete and debated (Beerling et al., 2002; Kürschner et al., 2001; Royer et al., 2001; Greenwood et al., 2003; Royer, 2003; Wing et al., 2005; Kato et al., 2011). Most *p*CO₂ estimates works have focused on the Paleocene–Eocene boundary (Beerling et al., 2002; Wing et al., 2005; Kato et al., 2011) and the middle Eocene (Deconto et al., 2012). In addition, the *p*CO₂ reconstruction results have varied based on different proxies. Various methods having been used in *p*CO₂ reconstruction mainly include the computer modeling methods: GEOCARB-I, GEOCARB-II, GEOCARB-III, GEOCARB-SULF and the proxies ice cores, paleosol carbonate, phytoplankton, nahcolite, Boron, and stomata parameters.

Generally, stomatal data (stomatal density and index) can be easily and accurately obtained from well-preserved fossil and modern leaves. Various plants showing the negative correlation between stomatal density (SD) or stomatal index (SI) and atmospheric CO₂ concentration have been used to reconstruct *p*CO₂, including *Ginkgo* (Beerling et al., 2002; Royer, 2003; Retallack, 2001, 2009a; Smith et al., 2010), *Metasequoia* (Royer, 2003; Doria et al., 2011), *Taxodium* (Stults et al., 2011), *Betula* (Kürschner et al., 2001; Sun et al., 2012), *Neolitsea* (Greenwood et al., 2003), *Quercus* (Kürschner et al., 1996, 2001) and multiple trees (Kürschner et al., 2008). Recently, positive correlations between stomatal index or stomatal frequency and *p*CO₂ have been reported based on fossil *Typha* and *Quercus* (Bai et al., 2015; Hu et al., 2015). However, the tropical and subtropical moist broadleaf forest conifer tree *Nageia* has been overlooked in paleobotanical estimates of *p*CO₂ concentration.

CPD

11, 2615–2647, 2015

The *p*CO₂ estimates of the late Eocene in South China

X.-Y. Liu et al.

Title Page

Abstract

Introduction

Conclusions

References

Tables

Figures



Back

Close

Full Screen / Esc

Printer-friendly Version

Interactive Discussion



Herein, we firstly document the correlation between the SD and SI of extant *Nageia motleyi* (Parl.) De Laub. leaves and atmospheric CO₂ concentration to provide a training dataset for application to fossil representatives. Furthermore, we estimate a new pCO₂ level for the late Eocene using the stomatal density method based on fossil *Nageia* from the late Eocene of South China, providing significant implications on discussing the climate change rhythm throughout the Eocene.

2 Background

2.1 Stomatal proxy in pCO₂ research

Stomatal proxy is widely used in reconstructions of pCO₂ concentration. The main parameters are stomatal density (SD) which is expressed as the total number of stomata divided by area, epidermal density (ED) expressed as the total number of epidermal cells per area and stomatal index (SI) calculated by the calculating the percentage of stomata among the total number of cells within an area [$SI = SD \times 100 / (SD + ED)$]. Woodward (1987) considered that both SD and SI had inverse relationships with atmospheric CO₂ during the development of the leaves. Subsequently, McElwain (1998) created the stomatal ratio (SR) method to reconstruct pCO₂. SR is a ratio of the stomatal density or index of a fossil [$SD_{(f)}$ or $SI_{(f)}$] to that of corresponding nearest living equivalent [$SD_{(e)}$ or $SI_{(e)}$], expressed as follows:

$$SR = SI_{(e)} / SI_{(f)} \quad (1)$$

The stomatal ratio method is a semiquantitative method of reconstructing pCO₂ concentrations under certain standardizations. One is the “carboniferous standardization” (Chaloner and McElwain, 1997) indicating that one stomatal ratio unit was equal to two RCO₂ units and:

$$SR = 2RCO_2 \quad (2)$$

CPD

11, 2615–2647, 2015

The pCO₂ estimates of the late Eocene in South China

X.-Y. Liu et al.

Title Page

Abstract

Introduction

Conclusions

References

Tables

Figures

◀

▶

◀

▶

Back

Close

Full Screen / Esc

Printer-friendly Version

Interactive Discussion



Where the value of RCO_2 is the pCO_2 level divided by the pre-industrial atmospheric level (PIL) of 300 ppm (McElwain, 1998) or that of the year when the NLE was collected (Berner, 1994; McElwain, 1998):

$$RCO_2 = C_{(f)}/300 \text{ or } RCO_2 = C_{(f)}/C_{(e)} \quad (3)$$

5 Then the estimated pCO_2 level is expressed as follows:

$$C_{(f)} = 0.5 \times C_{(e)} \times SD_{(e)}/SD_{(f)} \text{ or } C_{(f)} = 0.5 \times C_{(e)} \times SI_{(e)}/SI_{(f)} \quad (4)$$

Where $C_{(f)}$ is the pCO_2 and $C_{(e)}$ is the atmospheric CO_2 of the year when the NLE species was collected (McElwain and Chaloner, 1995, 1996; McElwain 1998). The equation adapts to the pCO_2 concentration prior to Cenozoic era.

10 Another standardization, the “Recent standardization” (McElwain, 1998), is expressed as one stomatal ratio unit being equal to one RCO_2 unit:

$$SR = 1RCO_2 \quad (5)$$

According to the equations stated above, the pCO_2 concentration can be expressed as:

$$15 C_{(f)} = C_{(e)} \times SD_{(e)}/SD_{(f)} \text{ or } C_{(f)} = C_{(e)} \times SI_{(e)}/SI_{(f)} \quad (6)$$

Where $C_{(f)}$, $C_{(e)}$, $SD_{(e)}$, $SD_{(f)}$, $SI_{(e)}$ and $SI_{(f)}$ are stated above. This standardization is usually used for reconstruction based on Cenozoic fossils (Chaloner and McElwain, 1997; McElwain, 1998; Beerling and Royer, 2002).

2.2 Review of extant and fossil *Nageia*

20 The genus *Nageia* including only seven living species, is an special group of Podocarpaceae which is a large family of conifers mainly distributed in the Southern

The pCO_2 estimates of the late Eocene in South China

X.-Y. Liu et al.

Title Page

Abstract

Introduction

Conclusions

References

Tables

Figures



Back

Close

Full Screen / Esc

Printer-friendly Version

Interactive Discussion



The $p\text{CO}_2$ estimates of the late Eocene in South China

X.-Y. Liu et al.

Title Page

Abstract

Introduction

Conclusions

References

Tables

Figures



Back

Close

Full Screen / Esc

Printer-friendly Version

Interactive Discussion



Hemisphere with broadly ovate-elliptic to oblong-lanceolate, multiveined (without a mid-vein), spirally arranged or in decussate, and opposite or subopposite leaves (Cheng et al., 1978; Fu et al., 1999). Generally, *Nageia* is divided into *Nageia* Sect. *Nageia* and *Nageia* Sect. *Dammaroideae* (Mill, 1999, 2001), mainly distributed in eastern Asia from north latitude 30° to nearly the equator and coastal mountain areas and island areas of the western Pacific Ocean, including South China, South Japan, Malaya and Indonesia, New Guinea, and other Pacific islands (Fu, 1992; Fig. 1a). Four species, ie., *Nageia nagi* (Thunberg) O. Kuntze, *N. fleuryi* (Hickel) De Laub., *N. formosensis* (Dummer) C. N. Page, and *N. nankoensis* (Hayata) R. R. Mill, of the *N.* section *Nageia*, have hypostomatic (the stomata only distributed on the abaxial side) leaves, with a single exception of *N. maxima* (De Laub.). De Laub. which is characterized by amphistomatic leaves but only a few stomata on the adaxial side (Hill and Pole, 1992; Sun, 2008). Both *N. wallichiana* (Presl) O. Kuntze and *N. motleyi*, of the *N.* section *Dammaroideae*, are amphistomatic with abundant stomata distributed on both sides of the leaf, especially *N. motleyi* having approximately equal stomata on both surfaces (Hill and Pole, 1992; Sun, 2008).

The fossil records of *Nageia* can be traced back to the Cretaceous with the evidence from Far East Russia, Japan and Henan, China (Krassilov, 1965; Matsuo, 1977; Kimura et al., 1988; Yang, 1990) and be extended into the Eocene of Hainan Island and Guangdong (Maoming), South China (Jin et al., 2010; Liu et al., 2015; Fig. 1a). Although some of the *Nageia* fossil materials described above have well-preserved cuticles (eg. Jin et al., 2010; Liu et al., 2015), the above studies are mainly concentrated on the morphology, systematics and phytogeography.

Nageia maomingensis Jin et Liu was reported based on four leaves with well-preserved cuticles recovered from late Eocene of South China (Liu et al., 2015). Among the modern *Nageia* species mentioned above, *N. motleyi* was considered as the nearest extant living (NEL) species of *N. maomingensis* (Liu et al., 2015). Both *N. maomingensis* and *N. motleyi* are amphistomatic indicating that both upper and lower surfaces of the leaf are needed to estimate the $p\text{CO}_2$ concentration during the late Eocene.

and three part of concentrated nitric acid) for 30 min, rinsed in water, and then treated with 8 % KOH (up to 30 min) and the abaxial and adaxial cuticles were separated with a hair mounted on needle. Finally, the cuticles were stained by 1 % Safranin T alcoholic solution for 5 min, sealed with Neutral Balsam and observed under the LM.

3.2 Fossil leaf preparation

Four fossil leaves of *Nageia maomingensis* were recovered from the late Eocene of the Youganwo Formation (MMJ1-001) and the Huangniuling Formation (MMJ2-003, MMJ2-004 and MMJ3-003) of Maoming Basin, South China (Fig. 1b and c). Macrofossil cuticular fragments were taken from the middle part of each fossil leaf (Fig. 2c) and treated by Schulze's solution for approximately 1 h and 5–10 % KOH for 30 min (Ye, 1981). The cuticles were observed and photographed under a Carl Zeiss Axio Scope A1 light microscope (LM). All fossil specimens and cuticle slides are housed in the Museum of Biology of Sun Yat-sen University, Guangzhou, China.

3.3 Stomatal counting strategy and calculation methods

SD, ED and SI are counted based on analyzing the pictures taken with the light microscope (LM) using the standard sampling protocol, only counting those stomata touching or straddling the left-hand side and top including the corner between them, provided by Poole and Kürschner (1999; Fig. 2b and d). A total of 1116 pictures (200× magnification of Zeiss LM) of the cuticles from 9 leaves of *N. motleyi* were counted. Each counting field was 0.366 mm². In *Nageia maomingensis*, 112 views (400× magnification) of the abaxial side and 150 views (400× magnification) of the adaxial side of cuticles were counted with an area of 0.092 mm². None of the counting areas above overlapped and they were larger than the minimum area (0.03 mm²) for statistics (Poole and Kürschner, 1999). In this study, the stomatic data of both surfaces are applied in $p\text{CO}_2$ reconstruction because both our fossil species and the NLE species are amphistomatic.

CPD

11, 2615–2647, 2015

The $p\text{CO}_2$ estimates of the late Eocene in South China

X.-Y. Liu et al.

Title Page

Abstract

Introduction

Conclusions

References

Tables

Figures



Back

Close

Full Screen / Esc

Printer-friendly Version

Interactive Discussion



4 Results

4.1 Correlations between the CO₂ concentrations and stomatal parameters of *Nageia motleyi*

The SD and SI data of the adaxial sides of *N. motleyi* leaves are shown in Table 2. The SDs and SIs range from 45.89 to 78.6 (mm⁻²) and from 2.89 to 3.94 (%), respectively. However, the SDs and SIs data of the abaxial sides, summarized in Table 3, give significantly higher values (53.22–82.71 in SDs and 3.13–4.66 in SIs) than those from the adaxial sides. Figure 3 shows the relationships between the stomatal parameters (SD and SI) of modern *N. motleyi* and the atmospheric CO₂ concentration (SD-CO₂ relationships and SI-CO₂ relationships). R² values in the SD- CO₂ relationships from both the adaxial and abaxial surfaces of *N. motleyi* are up to 0.841 and 0.725 (Fig. 3a and b), suggesting that the stomatal densities of *N. motleyi* are in significant inverse proportion to the CO₂ concentrations. However, the Fig. 3c and d indicate no relationships between the SIs and CO₂ concentrations for the extremely low level of the R² values (0.003 and 0.0608).

According to the results stated above, the stomatal ratio method can be used in estimating *p*CO₂ concentration of the late Eocene based on the stomatal densities (SDs) of the fossil species *N. maomingensis* and the extant species *N. motleyi*. Beerling (1999) and Royer (2001) considered both the SD and SI vary with economical and biological factors such as irradiance, temperature, and water supply, but the SI is more sensitive than the SD to the concentration of atmospheric CO₂ (Beerling, 1999) and more accurate in responding to the variation of *p*CO₂ concentration (Royer, 2001). However, the study of Kouwenberg et al. (2003) indicated that the SD better reflects the negative relationships with atmospheric CO₂ concentration.

The SD results of specimen No. 40 798 are closest to the fitted equations in Fig. 3a and b and therefore are selected to reconstruct the *p*CO₂ concentration. The specimen was collected by J. Sinclair and Salleh Kiah Bin from Gunong Tebu Forest Reserve,

CPD

11, 2615–2647, 2015

The *p*CO₂ estimates of the late Eocene in South China

X.-Y. Liu et al.

Title Page

Abstract

Introduction

Conclusions

References

Tables

Figures



Back

Close

Full Screen / Esc

Printer-friendly Version

Interactive Discussion



Malaysia, in 1955 at an altitude of 51 m and a CO₂ concentration of 313.73 ppmv during that time (Brown, 2010). Therefore, the SD from the adaxial and abaxial surfaces of *N. maomingensis* and its NLE species *N. motleyi* are used to recover *p*CO₂ concentrations based on the stomatal ratio method.

4.2 Stomatal parameters and *p*CO₂ estimates results

After being projected into a long-term carbon cycle model (GEOCARB III; Berner and Kothavalá, 2001), the results of this study compares well with the CO₂ concentrations for corresponding age within their error ranges (Fig. 4). The summary of stomatal parameters of the extant and fossil *Nageia* and reconstruction results are provided in Tables 2 and 3, respectively. SD and SI values were calculated for all samples of the extant and fossil *Nageia*. The mean SD and SI values of the adaxial surface are 44.5 ± 2.9 and 1.80 ± 0.12 , respectively (Table 5). The mean SD values of the abaxial and abaxial surface are 48.9 ± 3.0 and 53.22 ± 2.2 , respectively (Table 2 and 3). The mean SR values of both sides are quite similar with 1.24 ± 0.13 in adaxial side and 1.23 ± 0.09 in abaxial side (Tables 4 and 5). The average reconstruction results of *p*CO₂ concentration in the late Eocene of Maoming Basin is 391.0 ± 41.1 ppmv (Table 4) and 386.5 ± 27.8 ppmv (Table 5) with a 95% confidence interval based on the adaxial and abaxial cuticles, respectively. Clearly the two estimates are rather similar with a difference of 5 ppmv in mean value, which is clearly less than their own standard error, indicating that the reconstructions based on both sides are consistent in this fossil species. Table 4 shows gradually increasing *p*CO₂ level from the lower layer to the upper ones, while the *p*CO₂ estimated results based on the abaxial side are random with the highest result in lowest layer (Table 5).

The partial pressure of CO₂ decreases with elevation (Gale, 1972). Jones (1992) proposed that the relationship between elevation and partial pressure in the lower atmosphere can be expressed as $P = -10.6E + 100$, where *E* is elevation in kilometers and *P* is the percentage of partial pressure relative to sea level. Various studies corroborate that SI and SD of many plants have positive correlations with altitude (Körner

The *p*CO₂ estimates of the late Eocene in South China

X.-Y. Liu et al.

Title Page

Abstract

Introduction

Conclusions

References

Tables

Figures



Back

Close

Full Screen / Esc

Printer-friendly Version

Interactive Discussion



and Cochrane, 1985; Woodward, 1986; Woodward and Bazzaz, 1988; Beerling et al., 1992; Rundgren and Beerling, 1999) while they are negatively related to the partial pressure of CO₂ (Woodward and Bazzaz, 1988). Therefore, it is essential to take elevation calibration into account during the *p*CO₂ concentration estimates. However, Royer (2003) pointed out that it is unnecessary make this conversion when the trees lived at < 250 m in elevation. In this paper, the nearest living equivalent species, *Nageia motleyi*, grows at 51 m in elevation with *P* = 99.5, suggesting that CO₂ concentration estimates were only underestimated by 0.5%. Consequently, no correction is needed for the reconstruction result in this study.

5 Discussion

5.1 Paleoclimate reconstructed history

The *p*CO₂ throughout the Cenozoic was relatively lower than the levels through the Cretaceous (Ekart et al., 1999), but it is had an overall decreasing trend with some significantly changes on short-time scales (eg. in the earliest Eocene and middle Miocene Zachos et al., 2001; Wing et al., 2005; Lowenstein and Demicco, 2006; Fletcher et al., 2008; Zachos et al., 2008; Bijl et al., 2010; Kato et al., 2011). There is a wide range in *p*CO₂ estimates for the Paleogene, reflecting both problems in the various proxies. Both the fractionation of carbon isotopes by phytoplankton (Freeman and Hayes, 1992) and analysis of paleosol (fossil soil) carbonates (Ekart et al., 1999) demonstrate that carbon dioxide levels were less than 1000 ppmv before the Cretaceous–Tertiary boundary and have been decreasing since the Paleocene.

Based on the measurements of palaeosol carbon isotopes, Cerling (1991) reported that *p*CO₂ levels for the Eocene and Miocene through to the present was lower than 700 ppmv. Fletcher et al. (2008) also showed that an atmospheric CO₂ levels of approximately 680 ppmv by 60 million years ago. However, Stott (1992) reconstructed *p*CO₂ as 450–550 ppmv for the early Eocene based on phytoplankton. Additionally, the re-

CPD

11, 2615–2647, 2015

The *p*CO₂ estimates of the late Eocene in South China

X.-Y. Liu et al.

Title Page

Abstract

Introduction

Conclusions

References

Tables

Figures



Back

Close

Full Screen / Esc

Printer-friendly Version

Interactive Discussion



Beerling and Royer, 2011). Subsequently, the CO₂ concentration decreased gradually and reached 280 ppmv until the period of the industrial revolution (Fig. 5). Since then, however, the CO₂ concentration rebounded.

In conclusion, although various results were made by different *p*CO₂ reconstruction proxies at the same time, their entire decreasing tendency of *p*CO₂ level are remarkably consistent with each other since the Eocene (Fig. 5). Furthermore, during the Eocene the temperature was higher than at present. The reconstructed *p*CO₂ concentration based on the SD of fossil *Nageia* are 391.0 ± 41.1 ppmv and 386.5 ± 27.8 ppmv, showing a remarkably low *p*CO₂ level during the early late Eocene.

5.2 Implications from *Nageia motleyi* ecology

Nageia motleyi is restrictedly distributed in the southern half of Malay Peninsula, adjacent Sumatra, and southern Borneo (Fig. 1a) with the mean annual temperature of ca. 25–30 °C which is higher than South China (ca. 20–25 °C; Fig. 1a). This species is generally scattered in the canopy of primary and secondary rainforests on massive substrates and situations from well-drained, even arid, slopes to waterlogged peat swamps at elevations of 15–500 (~ 1000) m (Eckenwalder, 2009) and in Borneo surviving where there is deep peat in a mixed ramin-peat swamp, ridges, and hill sides in bindang-dipterocarp forest, and 1000 m on podsolic sandy loam (Coomes and Bellingham, 2011). All the living ecological characteristics of *N. motleyi* provide a significant implication that the temperature during the late Eocene might have been similar to that in the area where *N. motleyi* grows today.

Palynological assemblages from the late Eocene of Maoming Basin of Guangdong (Aleksandrova et al., 2012) suggest that the Youganwo Formation was humid, and the Huangniuling Formation had an increase of average annual temperatures and humidity during this period. Additionally, according to the winged-fruits *Shorea maomingensis* Feng, Kodrul et Jin (Dipterocarpaceae) recovered from the late Eocene of the Huangniuling Formation of the Maoming Basin and the living conditions of modern *Shorea*,

CPD

11, 2615–2647, 2015

The *p*CO₂ estimates of the late Eocene in South China

X.-Y. Liu et al.

Title Page

Abstract

Introduction

Conclusions

References

Tables

Figures



Back

Close

Full Screen / Esc

Printer-friendly Version

Interactive Discussion



Feng et al. (2013) point out the occurrence of seasonally dry climate at that time and a temperature higher than today.

In this article, we reconstructed the $p\text{CO}_2$ of the late Eocene as 391.0 ± 41.1 ppmv and 386.5 ± 27.8 ppmv, which are distinctly higher than the CO_2 level of 289.23–313.73 ppmv from extant leaves collected from 1968 to 1955 (Table 1), but similar to the extant CO_2 concentration of 387.35–401.52 ppmv from 2009 to 2015 (Brown, 2010; Pieter and Keeling, 2015). Compares with the reconstruction results in Fig. 5, our estimates show comparatively low $p\text{CO}_2$ concentration during the late Eocene. Combined with the low $p\text{CO}_2$ and the living conditions of *N. sect. Dammaroideae* (adapted to warm areas of East Asia) (Fig. 1), we conclude that the other factors may have played a role in the global climate changing process. Owing to the totally decreasing trend of the global climate change from the late Eocene reconstructed based on the proxies of stomata, paleosols, phytoplankton and B/Ca (Fig. 5), the plants of *N. Sect. Demmaroideae* migrated toward south and ultimately disappeared from South China (Fig. 1).

6 Conclusions

The stomatal data analysis suggests only the stomatal densities from both sides of *Nageia motleyi* leaves have significant negative correlations with the atmospheric CO_2 concentration, suggesting that we can estimate the $p\text{CO}_2$ of the Eocene in South China based on the stomatal densities of the Eocene fossil leaves of *N. maomingensis* and their nearest living equivalent species *N. motleyi*. Based on the stomatal ratio method, $p\text{CO}_2$ concentration of the late Eocene of Maoming Basin, Guangdong Province, is reconstructed as 391.0 ± 41.1 ppmv (based on the adaxial side of leaf cuticles) and 386.5 ± 27.8 ppmv (based on the abaxial side of leaf cuticles), showing low $p\text{CO}_2$ levels during the globally warm epoch of the Eocene, which is significantly higher than the historical CO_2 concentrations from 1868 to 1955 (around the industrial atmospheric level, 300 ppmv) and similar to the concentration of today.

The $p\text{CO}_2$ estimates of the late Eocene in South China

X.-Y. Liu et al.

Title Page

Abstract

Introduction

Conclusions

References

Tables

Figures



Back

Close

Full Screen / Esc

Printer-friendly Version

Interactive Discussion



Acknowledgements. This study was supported by the National Natural Science Foundation of China (Grant No. 41210001), the National Basic Research Program of China (973 Program) (Grant No. 2012CB822003), State Key Laboratory of Palaeobiology and Stratigraphy (Nanjing Institute of Geology and Palaeontology, CAS) (Grant No. 123110), the Fundamental Research Funds for the Central Universities (Grant No.12lgjc04), the Guangdong Provincial Natural Science Foundation of China (Grant No.10151027501000020), the Key Project of Sun Yat-sen University for inviting foreign teachers, the Scientific Research Fund, Hongda Zhang, Sun Yat-sen University, and the State Scholarship Fund of China Scholarship Council (CSC) (File No. 201306380046). We greatly thank the Sun Yet-sen (SYS) University Herbarium and the Herbarium of the V.L. Komarov Botanical Institute of the Russian Academy of Sciences (LE) for their permission to examine and collect extant *Nageia* specimens. We also express sincere gratitude to Prof. Sun Tongxing (Yancheng Teachers University), Dr. David Boufford (Harvard University) and Dr. Richard Chung Cheng Kong (Forest Research Institute Malaysia) for providing extant *N. motleyi* leaves from the herbarium of the Royal Botanic Garden at Edinburgh (E), the Harvard University Herbaria (A/GH) and the herbarium of Forest Research Institute Malaysia (KEP). We sincerely appreciate the guidance of Chengqian Wang (Harbin Institute of Technology) on preparing Figs. 3–5. We also offer sincere gratitude to Professor Steven Manchester and Ms. Margaret Joyner (US) for editing.

References

- Aleksandrova, G. N., Kodrul, T. M., Liu, X. Y., Song, Y. S., and Jin, J. H.: Palynological characteristics of the upper part of the Youganwo Formation and lower part of the Huangniuling Formation, Maoming Basin, South China, in: Proceedings, The 2nd Sino-Russian Seminar on Evolution and Development of Eastern Asia Flora based on Palaeobotanical Data, Sun Yat-sen University, Guangzhou, China, 3–15, 2012.
- Bai, Y. J., Chen, L. Q., Ranhotra, S. P., Wang, Q., Wang, Y. F., and Li, C. S.: Reconstructing atmospheric CO₂ during the Plio–Pleistocene transition by fossil *Typha*, Glob. Change Biol., 21, 874–881, doi:10.1111/gcb.12670, 2015.

The $p\text{CO}_2$ estimates of the late Eocene in South China

X.-Y. Liu et al.

Title Page

Abstract

Introduction

Conclusions

References

Tables

Figures



Back

Close

Full Screen / Esc

Printer-friendly Version

Interactive Discussion



The $p\text{CO}_2$ estimates of the late Eocene in South China

X.-Y. Liu et al.

Title Page

Abstract

Introduction

Conclusions

References

Tables

Figures



Back

Close

Full Screen / Esc

Printer-friendly Version

Interactive Discussion



- Barnett, T. P., Pierce, D. W., and Schnur, R.: Detection of anthropogenic climate change in the world's oceans, *Science*, 292, 270–274, doi:10.1126/science.1058304, 2001.
- Beerling, D. J.: Stomatal density and index: theory and application, in: *Fossil Plants and Spores: Modern Techniques*, edited by: Jones, T. P. and Rowe, N. P., Geological Society, London, 251–256, 1999.
- 5 Beerling, D. J. and Royer, D. L.: Reading a CO_2 signal from fossil stomata, *New Phytol.*, 153, 387–397, doi:10.1046/j.0028-646X.2001.00335.x, 2002.
- Beerling, D. J. and Royer, D. L.: Convergent Cenozoic CO_2 history, *Nat. Geosci.*, 4, 418–420, doi:10.1038/ngeo1186, 2011.
- 10 Beerling, D. J., Chaloner, W. G., Huntley, B., Pearson, J. A., Tooley, M. J., and Woodward, F. I.: Variations in the stomatal density of *Salix herbacea* L. under the changing atmospheric CO_2 concentrations of late- and post-glacial time, *Philos. T. R. Soc. Lon. B*, 336, 215–224, doi:10.1098/rstb.1992.0057, 1992.
- Beerling, D. J., Lomax, B. H., Royer, D. L., Upchurch Jr., G. R., and Kump, L. R.: An atmospheric $p\text{CO}_2$ reconstruction across the Cretaceous-Tertiary boundary from leaf megafossils, *P. Natl. Acad. Sci. USA*, 99, 7836–7840, doi:10.1073/pnas.122573099, 2002.
- Berner, R. A.: GEOCARB II: A revised model of atmospheric CO_2 over Phanerozoic time, *Am. J. Sci.*, 294, 56–91, doi:10.2475/ajs.294.1.56, 1994.
- 15 Berner, R. A. and Kothavalá, Z.: GEOCARB III: A revised model of atmospheric CO_2 over Phanerozoic time, *Am. J. Sci.*, 301, 182–204, doi:10.2475/ajs.301.2.182, 2001.
- Bijl, P. K., Houben, A. J. P., Schouten, S., Bohaty, S. M., Sluijs, A., Reichert, G., Sinninghe Damsté, J. S., and Brinkhuis, H.: Transient middle Eocene atmospheric CO_2 and temperature variations, *Science*, 330, 819–821, doi:10.1126/science.1193654, 2010.
- Brown, L. R.: Atmospheric carbon dioxide concentration, 1000–2009 (Supporting data), in: *World on the Edge: How to Prevent Environmental and Economic Collapse*. Chapter 4 Data: Rising Temperatures, Melting Ice, and Food Security, edited by: Brown, L. R., Earth Policy Institute, Norton, W. W. and Company, New York, London, available at: http://www.earth-policy.org/books/wote/wote_data, 2010.
- 25 Cerling, T. E.: Carbon dioxide in the atmosphere: evidence from Cenozoic and Mesozoic palaeosols, *Am. J. Sci.*, 291, 377–400, doi:10.2475/ajs.291.4.377, 1991.
- 30 Cerling, T. E.: Use of carbon isotopes in paleosols as an indicator of the $P(\text{CO}_2)$ of the paleoatmosphere, *Global Biogeochem. Cy.*, 6, 307–314, doi:10.1029/92GB01102, 1992.

The $p\text{CO}_2$ estimates of the late Eocene in South China

X.-Y. Liu et al.

Title Page

Abstract

Introduction

Conclusions

References

Tables

Figures



Back

Close

Full Screen / Esc

Printer-friendly Version

Interactive Discussion



- Chaloner, W. G. and McElwain, J. C.: The fossil plant record and global climate change, *Rev. Palaeobot. Palyno.*, 95, 73–82, doi:10.1016/S0034-6667(96)00028-0, 1997.
- Cheng, W. C., Fu, L. K., and Chao, C. S.: *Podocarpus* (Podocarpaceae), in: *Flora of China*, edited by: Cheng, W. and Fu, L., Science Press, Beijing, 7, 398–422, 1978 (in Chinese).
- 5 Coomes, D. A. and Bellingham, P. J.: Temperate and tropical podocarps: how ecologically alike are they, *Smithsonian Contrib. Bot.*, 95, 119–140, doi:10.5479/si.0081024X.95.119, 2011.
- Crowley, T. J.: Causes of climate change over the past 1000 years, *Science*, 289, 270–277, doi:10.1126/science.289.5477.270, 2000.
- DeConto, R. M., Galeotti, S., Pagani, M., Tracy, D., Schaefer, K., Zhang, T. J., Pollard, D., and Beerling, D. J.: Past extreme warming events linked to massive carbon release from thawing permafrost, *Nature*, 484, 87–91, doi:10.1038/nature10929, 2012.
- 10 Doria, G., Royer, D. L., Wolfe, A. P., Fox, A., Westgate, J. A., and Beerling, D. J.: Declining atmospheric CO_2 during the late Middle Eocene climate transition, *Am. J. Sci.*, 311, 63–75, doi:10.2475/01.2011.03, 2011.
- 15 Eckenwalder, J. E.: *Conifers of the World: the Complete Reference*, Timber Press, Portland London, 352–357, 2009.
- Ekart, D. D., Cerling, T. E., Montanez, I. P., and Tabor, N. J.: A 400 million year carbon isotope record of pedogenic carbonate: implications for paleoatmospheric carbon dioxide, *Am. J. Sci.*, 299, 805–827, doi:10.2475/ajs.299.10.805, 1999.
- 20 Feng, X. X., Tang, B., Kodual, T. M., and Jin, J. H.: Winged fruits and associated leaves of *Shorea* (Dipterocarpaceae) from the late Eocene of South China and their phylogeographic and paleoclimatic implications, *Am. J. Bot.*, 100, 574–581, doi:10.3732/ajb.1200397, 2013.
- Fletcher, B. J., Brentnall, S. J., Anderson, C. W., Berner, R. A., and Beerling, D. J.: Atmospheric carbon dioxide linked with Mesozoic and early Cenozoic climate change, *Nat. Geosci.*, 1, 43–48, doi:10.1038/ngeo.2007.29, 2008.
- 25 Freeman, K. H. and Hayes, J. M.: Fractionation of carbon isotopes by phytoplankton and estimates of ancient CO_2 levels, *Global Biogeochem. Cy.*, 6, 185–198, doi:10.1029/92GB00190, 1992.
- Fu, D. Z.: *Nageiaceae* – a new gymnosperm family, *Acta Phytotaxon. Sin.*, 30, 515–528, 1992 (in Chinese with English summary).
- 30 Fu, L. K., Li, Y., and Mill, R. R.: Podocarpaceae, in: *Flora of China*, edited by: Wu, Z. Y. and Raven, P. H., Science Press, Beijing, 4, 78–84, 1999.

The $p\text{CO}_2$ estimates of the late Eocene in South China

X.-Y. Liu et al.

Title Page

Abstract

Introduction

Conclusions

References

Tables

Figures



Back

Close

Full Screen / Esc

Printer-friendly Version

Interactive Discussion



- Gale, J.: Availability of carbon dioxide for photosynthesis at high altitudes: theoretical considerations, *Ecology*, 53, 494–497, doi:10.2307/1934239, 1972.
- Greenwood, D. G., Scarr, M. J., and Christophel, D. C.: Leaf stomatal frequency in the Australian tropical rain forest tree *Neolitsea dealbata* (Lauraceae) as a proxy measure of atmospheric $p\text{CO}_2$, *Palaeogeogr. Palaeoclimatol.*, 196, 375–393, doi:10.1016/S0031-0182(03)00465-6, 2003.
- 5 Harries, J. E., Brindley, H. E., Sagoo, P. J., and Bantges, R. J.: Increases in greenhouse forcing inferred from the outgoing long wave radiation spectra of the Earth in 1970 and 1997, *Nature*, 410, 355–357, doi:10.1038/35066553, 2001.
- Hill, R. S. and Pole, M. S.: Leaf and shoot morphology of extant *Afrocarpus*, *Nageia* and *Retrophyllum* (Podocarpaceae) species, and species with similar leaf arrangement, from Tertiary sediments in Australasia, *Aust. Syst. Bot.*, 5, 337–358, doi:10.1071/SB9920337, 1992.
- 10 Hu, J. J., Xing, Y. W., Turkington, R., Jacques, F. M. B. Su, T., Huang, Y. J., and Zhou, Z. K.: A new positive relationship between $p\text{CO}_2$ and stomatal frequency in *Quercus guyavifolia* (Fagaceae): a potential proxy for palaeo- CO_2 levels, *Ann. Bot.-London*, 115, 777–788, doi:10.1093/aob/mcv007, 2015.
- 15 Jacques, F. M. B., Shi, G. L., Li, H. M., and Wang, W. M.: An early-middle Eocene Antarctic summer monsoon: Evidence of “fossil climates”, *Gondwana Res.*, 25, 1422–1428, doi:10.1016/j.gr.2012.08.007, 2014.
- Jin, J. H., Qiu, J., Zhu, Y. A., and Kodrul, T. M.: First fossil record of the genus *Nageia* (Podocarpaceae) in South China and its phytogeographic implications, *Plant Syst. Evol.*, 285, 159–163, doi:10.1007/s00606-010-0267-4, 2010.
- 20 Jones, H. G.: *Plants and Microclimate*, Cambridge University Press, Cambridge, UK, 1–428, 1992.
- Kato, Y., Fujinaga, K., and Suzuki, K.: Marine Os isotopic fluctuations in the early Eocene greenhouse interval as recorded by metalliferous umbers from a Tertiary ophiolite in Japan, *Gondwana Res.*, 20, 594–607, doi:10.1016/j.gr.2010.12.007, 2011.
- 25 Kimura, T., Ohana, T., and Mimoto, K.: Discovery of a podocarpaceous plant from the Lower Cretaceous of Kochi Prefecture, in the outer zone of southwest Japan, *P. Jpn. Acad. B-Phys.*, 64, 213–216, doi:10.2183/pjab.64.213, 1988.
- 30 Koch, P. L., Zachos, J. C., and Gingerich, P. D.: Correlation between isotope records in marine and continental carbon reservoirs near the Palaeocene/Eocene boundary, *Nature*, 358, 319–322, doi:10.1038/358319a0, 1992.

The $p\text{CO}_2$ estimates of the late Eocene in South China

X.-Y. Liu et al.

[Title Page](#)

[Abstract](#)

[Introduction](#)

[Conclusions](#)

[References](#)

[Tables](#)

[Figures](#)



[Back](#)

[Close](#)

[Full Screen / Esc](#)

[Printer-friendly Version](#)

[Interactive Discussion](#)



- Kouwenberg, L. L. R., McElwain, J. C., Kürschner, W. M., Wagner, F., Beerling, S. J., Mayle, F. E., and Visscher, H.: Stomatal frequency adjustment of four conifer species to historical changes in atmospheric CO_2 , *Am. J. Bot.*, 90, 610–619, 2003.
- Körner, Ch., and Cochrane, P. M.: Stomatal responses and water relations of *Eucalyptus pauciflora* in summer along an elevational gradient, *Oecologia*, 66, 443–455, doi:10.1007/BF00378313, 1985.
- Krassilov, V. A.: New coniferales from Lower Cretaceous of Primorye, *Bot. J.*, 50, 1450–1455, 1965 (in Russia).
- Kürschner, W. M., van der Burgh, J., Visscher, H., and Dilcher, D. L.: Oak leaves as biosensors of late Neogene and early Pleistocene paleoatmospheric CO_2 concentrations, *Mar. Micropaleontol.*, 27, 299–312, doi:10.1016/0377-8398(95)00067-4, 1996.
- Kürschner, W. M., Wagner, F., Dilcher, D. L., and Visscher, H.: Using fossil leaves for the reconstruction of Cenozoic paleoatmospheric CO_2 concentrations, in: *Geological Perspectives of Global Climate Change*, edited by: Gerhard, L. C., Harrison, W. E., and Hanson, B. M., APPG Studies in Geology, 47, Tulsa, 169–189, 2001.
- Kürschner, W. M., Kvaček, Z., and Dilcher, D. L.: The impact of Miocene atmospheric carbon dioxide fluctuations on climate and the evolution of terrestrial ecosystems, *P. Natl. Acad. Sci. USA*, 105, 449–453, doi:10.1073/pnas.0708588105, 2008.
- Levitus, S., Antonov, J. I., Wang, J., Delworth, T. L., Dixon, K. W., and Broccoli, A. J.: Anthropogenic warming of Earth's climate system, *Science*, 292, 267–270, doi:10.1126/science.1058154, 2001.
- Liu, X. Y., Gao, Q., and Jin, J. H.: late Eocene leaves of *Nageia Gaertner* (section *Dammaroideae* Mill) from Maoming Basin, South China and their implications on phytogeography, *J. Syst. Evol.*, 999, 1–11, doi:10.1111/jse.12133, 2015.
- Lowenstein, T. K. and Demicco, R. V.: Elevated Eocene atmospheric CO_2 and its subsequent decline, *Science*, 313, 1928, doi:10.1126/science.1129555, 2006.
- Mann, M. E., Bradley, R. S., and Hughes, M. K.: Global-scale temperature patterns and climate forcing over the past six centuries, *Nature*, 392, 779–787, doi:10.1038/33859, 1998.
- McElwain, J. C.: Do fossil plants signal palaeoatmospheric carbon dioxide concentration in the geological past, *Philos. T. R. Soc. Lon. B*, 353, 83–96, doi:10.1098/rstb.1998.0193, 1998.
- McElwain, J. C. and Chaloner, W. G.: Stomatal density and index of fossil plants track atmospheric carbon dioxide in the Palaeozoic, *Ann. Bot.-London*, 76, 389–395, doi:10.1006/anbo.1995.1112, 1995.

The $p\text{CO}_2$ estimates of the late Eocene in South China

X.-Y. Liu et al.

Title Page

Abstract

Introduction

Conclusions

References

Tables

Figures



Back

Close

Full Screen / Esc

Printer-friendly Version

Interactive Discussion



Mill, R. R.: A new combination in *Nageia* (Podocarpaceae), *Novon*, 9, 77–78, 1999.

Mill, R. R.: A new sectional combination in *Nageia* Gaertn (Podocarpaceae), *Edinburgh J. Bot.*, 58, 499–501, doi:10.1017/S0960428601000804, 2001.

Mitchell, J. F. B., Karoly, D. J., Hegerl, G. C., Zwiers, F. W., Allen, M. R., and Marengo, J.: Detection of climate change and attribution of causes, in: *Climate Change 2001: The Scientific Basis*, edited by: Houghton, J. T., Ding, Y. H., Griggs, D. J., Noguer, M., van der Linden, P. J., Dai, X. S., Maskell, K., and Johnson, C. A., Contribution of Working Group I to the Third Assessment Report of the Intergovernmental Panel on Climate Change: Cambridge University Press, Cambridge, UK, 1–881, 2001.

Matsuo, H.: Catalogue of Trees in Ishikawa Prefecture. Part 1. Fossil species. *Forestry Inst., Ishikawa Prefecture*, 35, 1977 (in Japanese).

Pagani, M., Zachos, J. C., Freeman, K. H., Tiplle, B., and Bohaty, S.: Marked decline in atmospheric carbon dioxide concentrations during the Paleocene, *Science*, 309, 600–603, doi:10.1126/science.1110063, 2005.

Pearson, P. N., Foster, G. L., and Wade, B. S.: Atmospheric carbon dioxide through the Eocene-Oligocene climate transition, *Nature*, 461, 1110–1113, doi:10.1038/nature08447, 2009.

Petit, J. R.: Climate and atmospheric history of the past 420,000 years from the Vostokicecore, Antarctica, *Nature*, 399, 429–436, doi:10.1038/20859, 1999.

Pieter, T. and Keeling, R.: Recent monthly average Mauna Loa CO_2 , NOAA/ESRL, available at: www.esrl.noaa.gov/gmd/ccgg/trends/, 2015.

Poole, I. and Kürschner, W. M.: Stomatal density and index: the practice, in: *Fossil Plants and Spores: Modern Techniques*, edited by: Jones, T. P. and Rowe, N. P., Geological Society, London, 257–260, 1999.

Retallack, G. J.: A 300-million-year record of atmospheric carbon dioxide from fossil plant cuticles, *Nature*, 411, 287–290, doi:10.1038/35077041, 2001.

Retallack, G. J.: Greenhouse crises of the past 300 million years, *Geol. Soc. Am. Bull.*, 121, 1441–1455, doi:10.1130/B26341.1, 2009a.

Retallack, G. J.: Refining a pedogenic-carbonate CO_2 paleobarometer to quantify a middle Miocene greenhouse spike, *Palaeogeogr. Palaeoclimatol.*, 281, 57–65, doi:10.1016/j.palaeo.2009.07.011, 2009b.

Roth-Nebelsicka, A., Utescher, T., Mosbrugger, V., Diester-Haass, L., and Walther, H.: Changes in atmospheric CO_2 concentrations and climate from the late Eocene to early Miocene:

The $p\text{CO}_2$ estimates of the late Eocene in South China

X.-Y. Liu et al.

Title Page

Abstract

Introduction

Conclusions

References

Tables

Figures



Back

Close

Full Screen / Esc

Printer-friendly Version

Interactive Discussion



palaeobotanical reconstruction based on fossil floras from Saxony, Germany, *Palaeogeogr. Palaeocl.*, 205, 43–67, doi:10.1016/j.palaeo.2003.11.014, 2004.

Royer, D. L.: Stomatal density and stomatal index as indicators of paleoatmospheric CO_2 concentration, *Rev. Palaeobot. Palynol.*, 114, 1–28, doi:10.1016/S0034-6667(00)00074-9, 2001.

Royer, D. L.: Estimating latest Cretaceous and Tertiary atmospheric CO_2 from stomatal indices, in: *Causes and Consequences of Globally Warm Climates in the early Paleocene*, edited by: Wing, S. L., Gingerich, P. D., Schmitz, B., and Thomas, E., Geological Society of America Special Paper, 79–93, 2003.

Royer, D. L.: CO_2 -forced climate thresholds during the Phanerozoic, *Geochim. Cosmochim. Ac.*, 70, 5665–5675, doi:10.1016/j.gca.2005.11.031, 2006.

Royer, D. L., Wing, S. L., Beerling, D. J., Jolley, D. W., Koch, P. L., Hickey, L. J., and Berner, R. A.: Paleobotanical evidence for near present-day levels of atmospheric CO_2 during part of the Tertiary, *Science*, 292, 2310–2313, doi:10.1126/science.292.5525.2310, 2001.

Rundgren, M. and Beerling, D. J.: A Holocene CO_2 record from the stomatal index of subfossil *Salix herbacea* L. leaves from northern Sweden, *Holocene*, 9, 509–513, doi:10.1191/095968399677717287, 1999.

Smith, R. Y., Greenwood, D. R., and Basinger, J. F.: Estimating paleoatmospheric $p\text{CO}_2$ during the early Eocene Climatic Optimum from stomatal frequency of *Ginkgo*, Okanagan Highlands, British Columbia, Canada, *Palaeogeogr. Palaeocl.*, 293, 120–131, doi:10.1016/j.palaeo.2010.05.006, 2010.

Stott, L. D.: Higher temperatures and lower oceanic $p\text{CO}_2$: A climate enigma at the end of the Paleocene Epoch, *Paleoceanography*, 7, 395–404, doi:10.1029/92PA01183, 1992.

Stults, D. Z., Wagner-Cremer, F., and Axsmith, B. J.: Atmospheric paleo- CO_2 estimates based on *Taxodium distichum* (Cupressaceae) fossils from the Miocene and Pliocene of Eastern North America, *Palaeogeogr. Palaeocl.*, 309, 327–332, doi:10.1016/j.palaeo.2011.06.017, 2011.

Sun, B. N., Ding, S. T., Wu, J. Y., Dong, C., Xie, S. P., and Lin, Z. C.: Carbon isotope and stomatal data of late Pliocene Betulaceae leaves from SW China: Implications for palaeoatmospheric CO_2 -levels, *Turk. J. Earth Sci.*, 21, 237–250, doi:10.3906/yer-1003-42, 2012.

Sun, T. X.: Cuticle micromorphology of *Nageia*, *J. Wuhan Bot. Res.*, 26, 554–560, doi:10.3969/j.issn.2095-0837.2008.06.002, 2008 (in Chinese with English abstract).

The $p\text{CO}_2$ estimates of the late Eocene in South China

X.-Y. Liu et al.

Title Page

Abstract

Introduction

Conclusions

References

Tables

Figures



Back

Close

Full Screen / Esc

Printer-friendly Version

Interactive Discussion



- Tripathi, A. K., Roberts, C. D., and Eagle, R. A.: Coupling of CO_2 and ice sheet stability over major climate transitions of the last 20 million years, *Science*, 326, 1394–1397, doi:10.1126/science.1178296, 2009.
- Wing, S. L.: Transient floral change and rapid global warming at the Paleocene–Eocene boundary, *Science*, 310, 993–996, 2005.
- 5 Woodward, F. I.: Ecophysiological studies on the shrub *Vaccinium myrtillus* L. taken from a wide altitudinal range, *Oecologia*, 70, 580–586, doi:10.1007/BF00379908, 1986.
- Woodward, F. I.: Stomatal numbers are sensitive to increases in CO_2 concentration from pre-industrial levels, *Nature*, 327, 617–618, doi:10.1038/327617a0, 1987.
- 10 Woodward, F. I. and Bazzaz, F. A.: The responses of stomatal density to CO_2 partial pressure, *J. Exp. Bot.*, 39, 1771–1781, doi:10.1093/jxb/39.12.1771, 1988.
- Yang, J. J., Qi, G. F., and Xu, R. H.: Studies on fossil woods excavated from the Dabie mountains, *Sci. Silvae Sinicae*, 26, 379–386, 1990 (in Chinese with English abstract).
- Zachos, J., Pagani, M., Sloan, L., Thomas, E., and Billups, K.: Trends, rhythms, aberrations in global climate 65 Ma to present, *Science*, 292, 686–693, doi:10.1126/science.1059412, 2001.
- 15

The $p\text{CO}_2$ estimates of the late Eocene in South China

X.-Y. Liu et al.

Table 3. Summary of stomatal parameters of the abaxial surface form modern *Nageia motleyi* (Parl.) De Laub.

| Collection number | Collection date | CO ₂ (ppmv) | SD (mm ⁻²) | | | | | SI (%) | | | | |
|-------------------|-----------------|------------------------|------------------------|----------|------|--------|-----|-----------|----------|------|--------|-----|
| | | | \bar{x} | σ | s.e. | t*s.e. | n | \bar{x} | σ | s.e. | t*s.e. | n |
| No.2649 | 1868 | 289.23 | 82.71 | 12.23 | 1.02 | 2.00 | 144 | 3.89 | 0.58 | 0.05 | 0.09 | 144 |
| No.bb.17 229 | 1932 | 306.19 | 69.16 | 14.23 | 1.48 | 2.90 | 93 | 3.13 | 0.58 | 0.06 | 0.12 | 93 |
| No.bb.18 328 | 1934 | 306.46 | 69.92 | 14.38 | 1.52 | 2.97 | 90 | 3.99 | 1.08 | 0.11 | 0.22 | 90 |
| No.bb.21 151 | 1936 | 306.76 | 75.68 | 15.74 | 1.66 | 3.25 | 90 | 4.66 | 0.88 | 0.09 | 0.18 | 90 |
| No.40 798 | 1955 | 313.73 | 53.22 | 13.88 | 1.12 | 2.19 | 155 | 3.71 | 0.93 | 0.07 | 0.15 | 155 |

Note: \bar{x} – mean; σ – standard deviation; s.e. – standard error of mean; n – numbers of photos counts (40x); t*s.e. – 95% confidence interval.

[Title Page](#)
[Abstract](#)
[Introduction](#)
[Conclusions](#)
[References](#)
[Tables](#)
[Figures](#)

[Back](#)
[Close](#)
[Full Screen / Esc](#)
[Printer-friendly Version](#)
[Interactive Discussion](#)


The $p\text{CO}_2$ estimates of the late Eocene in South China

X.-Y. Liu et al.

Table 4. Summary of stomatal parameters of the adaxial surface of fossil *Nageia* and $p\text{CO}_2$ [$C_{(f)}$] estimates results.

| Species | Age | SD (mm^{-2}) | | | | SI (%) | | | | SR | | $C_{(f)}$ (ppmv) | |
|-----------|-------------|-------------------------|----------|------|-----|--------|----------|------|-----|------|-------|------------------|-------|
| | | x | σ | s.e. | n | x | σ | s.e. | n | x | t*s.e | x | t*s.e |
| MMJ1-001 | late Eocene | 52.5 | 17.1 | 3.1 | 30 | 2.08 | 0.7 | 0.1 | 30 | 0.99 | 0.14 | 311.9 | 45.1 |
| MMJ2-003 | late Eocene | 42.3 | 12.9 | 2.4 | 30 | 1.80 | 0.6 | 0.1 | 30 | 1.29 | 0.29 | 405.7 | 91.8 |
| MMJ2-004 | late Eocene | 39.9 | 13.6 | 2.5 | 30 | 1.66 | 0.6 | 0.1 | 30 | 1.33 | 0.24 | 419.4 | 74.1 |
| MMJ3-003a | late Eocene | 43.2 | 17.7 | 3.2 | 30 | 1.67 | 0.7 | 0.1 | 30 | 1.36 | 0.31 | 427.2 | 98.7 |
| Mean | late Eocene | 44.5 | 16.3 | 1.5 | 120 | 1.80 | 0.7 | 0.1 | 120 | 1.24 | 0.13 | 391.0 | 41.1 |

Note: x – mean; σ – standard deviation; s.e. – standard error of mean; n – numbers of photos counts (400 \times); t*s.e. – 95% confidence interval.

Title Page

Abstract

Introduction

Conclusions

References

Tables

Figures



Back

Close

Full Screen / Esc

Printer-friendly Version

Interactive Discussion



The $p\text{CO}_2$ estimates of the late Eocene in South China

X.-Y. Liu et al.

Table 5. Summary of stomatal parameters of the abaxial surface of fossil *Nageia* and $p\text{CO}_2$ [$C_{(f)}$] estimates results.

| Species | Age | SD (mm^{-2}) | | | | SI (%) | | | | SR | | $C_{(f)}$ (ppmv) | |
|-----------|-------------|-------------------------|----------|------|-----|--------|----------|------|-----|------|-------|------------------|-------|
| | | x | σ | s.e. | n | x | σ | s.e. | n | x | t*s.e | x | t*s.e |
| MMJ1-001 | late Eocene | 47.7 | 17.7 | 3.2 | 30 | 2.11 | 0.8 | 0.2 | 30 | 1.28 | 0.18 | 401.8 | 56.4 |
| MMJ2-003 | late Eocene | 50.9 | 18.3 | 3.3 | 30 | 2.12 | 0.8 | 0.1 | 30 | 1.21 | 0.18 | 378.7 | 55.1 |
| MMJ2-004 | late Eocene | 48.2 | 15.8 | 2.9 | 30 | 2.14 | 0.7 | 0.1 | 30 | 1.25 | 0.19 | 393.2 | 60.2 |
| MMJ3-003a | late Eocene | 48.9 | 12.6 | 2.7 | 22 | 1.85 | 0.5 | 0.1 | 22 | 1.17 | 0.15 | 368.0 | 46.0 |
| Mean | late Eocene | 48.9 | 16.2 | 1.5 | 112 | 2.07 | 0.7 | 0.1 | 112 | 1.23 | 0.09 | 386.5 | 27.8 |

Note: x – mean; σ – standard deviation; s.e. – standard error of mean; n – numbers of photos counts (400 \times); t*s.e. – 95% confidence interval.

[Title Page](#)
[Abstract](#)
[Introduction](#)
[Conclusions](#)
[References](#)
[Tables](#)
[Figures](#)

[Back](#)
[Close](#)
[Full Screen / Esc](#)
[Printer-friendly Version](#)
[Interactive Discussion](#)

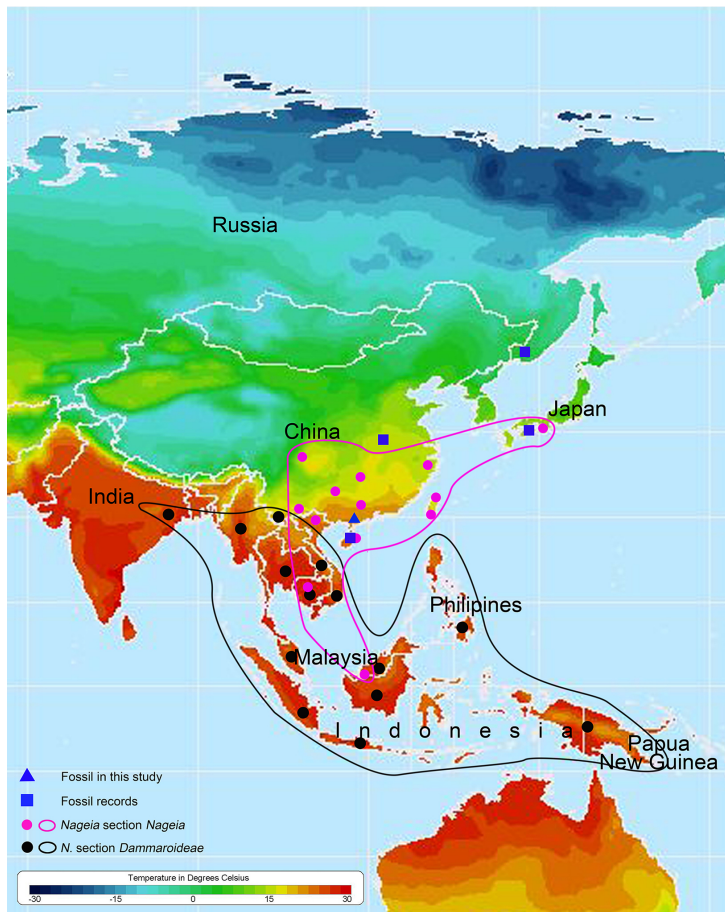



Figure 1. Map showing the distribution of extant and fossil *Nageia* and their mean annual temperature (Modified after the map from <http://nelson.wisc.edu/sage/data-and-models/atlas/maps.php?datasetid=35&includerelatedlinks=1&dataset=35>).

The $p\text{CO}_2$ estimates of the late Eocene in South China

X.-Y. Liu et al.

Title Page

Abstract Introduction

Conclusions References

Tables Figures

◀ ▶

◀ ▶

Back Close

Full Screen / Esc

Printer-friendly Version

Interactive Discussion



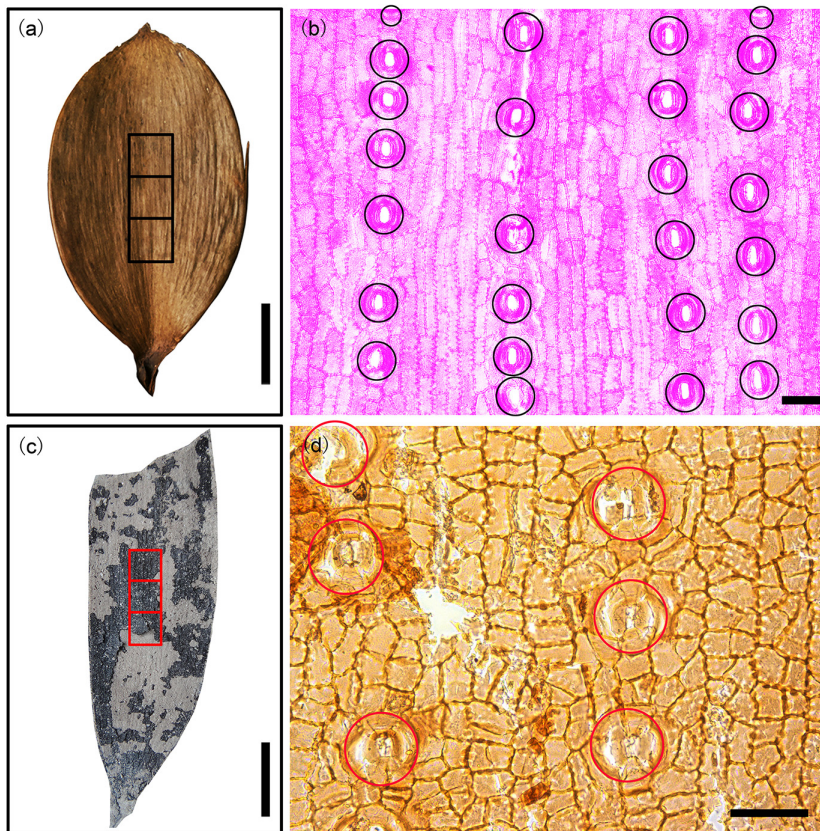


Figure 2. Sampling areas and counting rules are shown. **(a)** *Nageia motleyi* (Parl.) De Laub.leaf. Black squares in the middle of the leaf show the sampling areas for preparing the cuticles. **(b)** The abaxial side of the cuticle from *N. motleyi* leaf. Black circles show the counted stomatal complexes. **(c)** *N. maomingensis* Jin et Liu. Red squares in the middle of the leaf indicate the sampling areas. **(d)** The abaxial side of the fossil cuticle. Red circles show the counted stomatal complexes. Scale bars: **(a)** and **(c)** = 1 cm; **(b)** and **(d)** = 50 μ m.

Title Page

Abstract

Introduction

Conclusions

References

Tables

Figures

◀

▶

◀

▶

Back

Close

Full Screen / Esc

Printer-friendly Version

Interactive Discussion



The $p\text{CO}_2$ estimates of the late Eocene in South China

X.-Y. Liu et al.

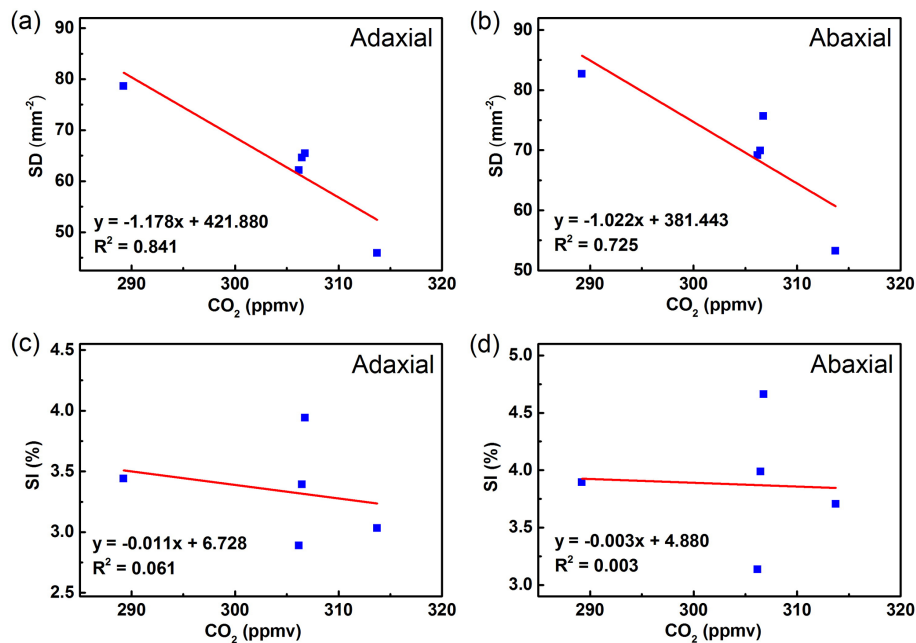


Figure 3. Correlation between SD and SI vs. CO₂ concentration for modern *Nageia motleyi*. **(a)** Trends of SD with CO₂ concentration for the adaxial surface. **(b)** Trends of SD with CO₂ concentration for the abaxial surface. **(c)** Trends of SI with CO₂ concentration for the adaxial surface. **(d)** Trends of SI with CO₂ concentration for the abaxial surface.

Title Page

Abstract

Introduction

Conclusions

References

Tables

Figures



Back

Close

Full Screen / Esc

Printer-friendly Version

Interactive Discussion



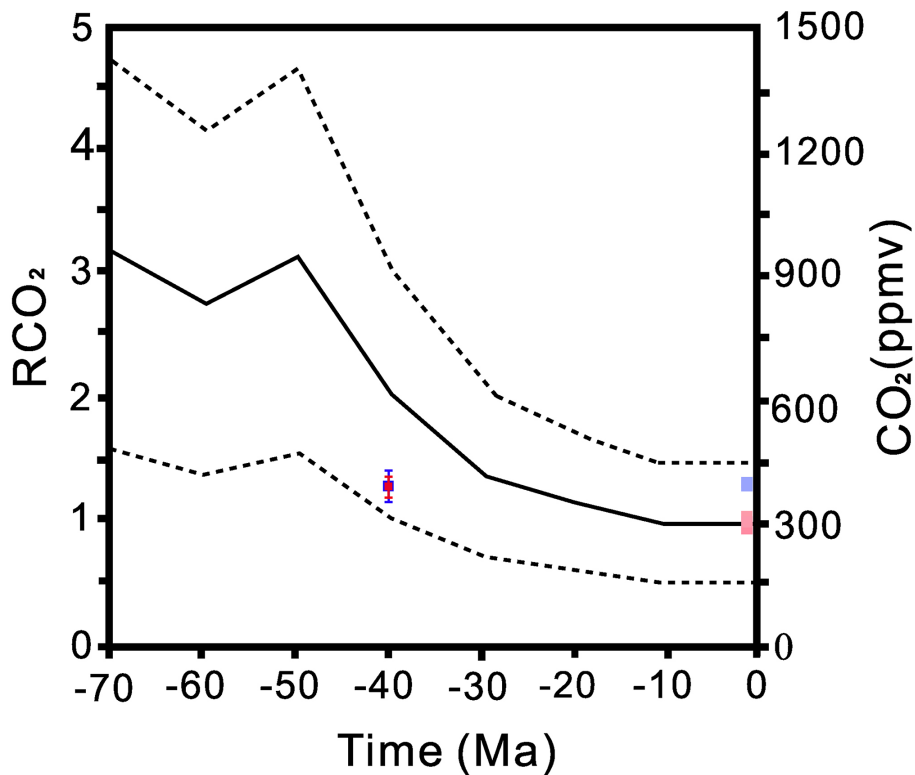


Figure 4. The pCO_2 reconstruction results and extant CO_2 concentrations are projected onto the long-term carbon cycle model (GEOCARB III; Berner and Kothavalá, 2001). The pCO_2 results based on the adaxial and abaxial surfaces are represented by blue and red, respectively. The CO_2 concentrations from 1968 to 1955 are shown by light red and those from 2009 to 2015 are in light blue (they are not the CO_2 concentrations of Holocene).

The pCO_2 estimates of the late Eocene in South China

X.-Y. Liu et al.

Title Page

Abstract

Introduction

Conclusions

References

Tables

Figures

◀

▶

◀

▶

Back

Close

Full Screen / Esc

Printer-friendly Version

Interactive Discussion



The $p\text{CO}_2$ estimates of the late Eocene in South China

X.-Y. Liu et al.

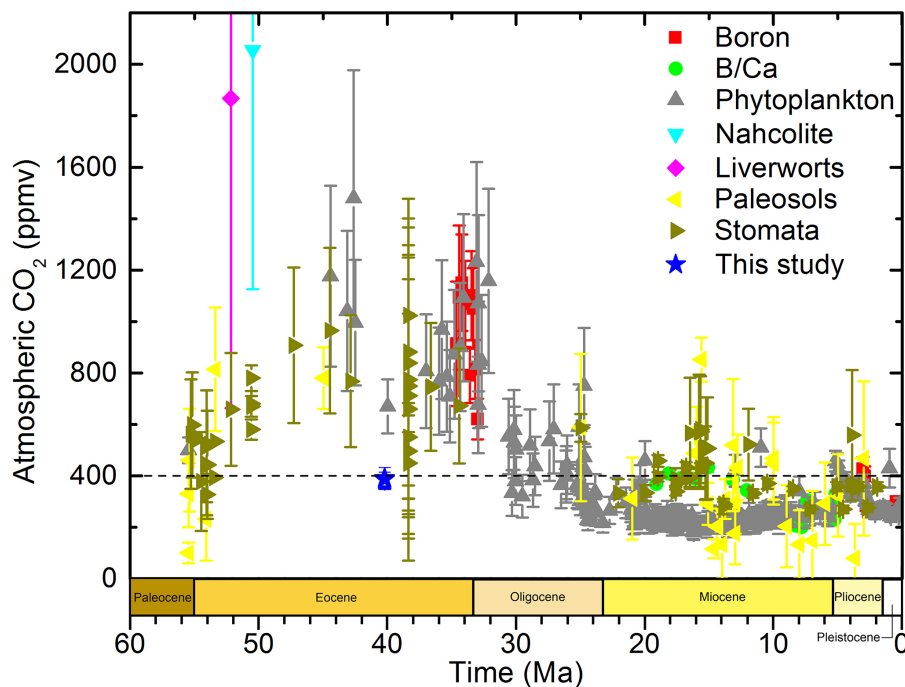


Figure 5. Atmospheric CO_2 estimates from proxies over the past 60 million years. The horizontal dashed line indicates monthly atmospheric CO_2 concentration for March 2015 at Mauna Loa, Hawaii (401.52 ppmv) (Pieter and Keeling, 2015). The vertical lines show the error bars. The data were from the supporting data of Beerling and Royer (2011) and the references in Table 6.

Title Page

Abstract

Introduction

Conclusions

References

Tables

Figures



Back

Close

Full Screen / Esc

Printer-friendly Version

Interactive Discussion

